Proc. Natl. Acad. Sci. USA
Vol. 76, No. 10, pp. 4867–4871, October 1979
Biochemistry

Quaternary structure of the ribosomal 30S subunit: Model and its experimental testing

(ribosome/ribosomal 16S RNA/ribosomal proteins/neutron scattering/electron microscopy)

ALEXANDER S. SPIRIN, IGOR N. SERDYUK, JOSEPH L. SHPUNGIN, AND VICTOR D. VASILIEV

Institute of Protein Research, Academy of Sciences of the U.S.S.R., Poustchino, Moscow Region, U.S.S.R.

Communicated by Israel M. Gelfand, June 26, 1979

ABSTRACT **In considering the structure of the 30S subunit of the *Escherichia coli* ribosome, we have assumed that: (*i*) all or almost all the proteins within the 30S particle are compact and globular, as recently shown for the isolated proteins S4, S7, S8, S15, and S16 in solution [Serdyuk, I. N., Zaccai, G. & Spirin, A. S. (1978) *FEBS Lett.* 94, 349–352]; (*ii*) the RNA within the 30S particle has approximately the same specific V-like or Y-like shape that was demonstrated for the isolated 16S RNA in a compact conformation [Vasiliev, V. D., Selivanova, O. M. & Koteliansky, V. E. (1978) *FEBS Lett.* 95, 273–276]. From these assumptions and using the numerous data reported on neighboring ribosomal proteins, we have constructed a model of the quaternary structure of the ribosomal 30S subunit. The model has been tested by calculation of the theoretical curves of neutron scattering at different contrasts, as well as those of x-ray scattering, and their comparison with the experimental scattering curves for *E. coli* 30S particles. It has been found that the calculated scattering curves for the model practically coincide with the experimental scattering curves for the 30S particles in the range of Bragg distances down to 40–55 Å. The scattering curves calculated for several three-dimensional patterns of arrangement of the 30S subunit proteins proposed earlier have been shown to be inconsistent with the experiments.**

In recent years, the technique of chemical crosslinking of neighboring proteins by bifunctional reagents and measurements of the distances between deuterated or fluorescent-labeled proteins by using neutron scattering or energy transfer techniques, respectively, have contributed much to the knowledge of the protein topography in ribosomal particles and especially in the ribosomal 30S subunit of *Escherichia coli*. From these and a number of less direct data, several models of the topography of ribosomal proteins in the 30S particle have been proposed (1–8). Independently, the use of the immunoelectron microscopy technique has also led to two different models of the topography of ribosomal proteins on the surface of the 30S particle (9–12; see also ref. 13).

However, two complications have hampered further progress. First, no information was available as to three-dimensional structure and morphology of the 16S RNA; this RNA is known to be a structural backbone for arrangement of ribosomal proteins. Second, immunoelectron microscopy (9, 10) and neutron scattering (14, 15) data on proteins within the 30S subunit, as well as some physical measurements of isolated ribosomal proteins (16–21), have suggested strongly elongated or very expanded shapes of many ribosomal proteins; this led to ambiguity in interpretation of the results on chemical crosslinking, energy transfer, etc.

Most recently, a specific compact conformation of the 16S RNA has been visualized by electron microscopy (22). On the other hand, a number of ribosomal proteins, such as S4, S7, S8, S15, and S16, have been reinvestigated and found to be compact globular proteins with cooperative tertiary structures (23–25). Based on these new results and using the numerous data reported on mutual arrangement (topography) of ribosomal proteins, we have constructed a model of the quaternary structure of the ribosomal 30S particle and then checked it by neutron and x-ray scattering experiments.

The publication costs of this article were defrayed in part by page charge payment. This article must therefore be hereby marked "*advertisement*" in accordance with 18 U. S. C. §1734 solely to indicate this fact.

MODEL CONSTRUCTION

Initial Assumptions. In constructing the model, we have adhered to the size and the asymmetric three-dimensional structure of the ribosomal 30S subunit first deduced by one of us from electron microscopy of freeze-dried and shadow-cast samples of the particles (26). Morphologically, the 30S particle was found to be subdivided into a "head," a "body," and a side "bulge" (Fig. 1). A similar subdivision of the 30S particles, with a side "platform," was reported also by Lake and Kahan (11) and Lake (27) on the basis of electron microscopy of negatively stained samples.

We have proceeded from two principal assumptions: (*i*) RNA within the 30S particle has a specific V-like or Y-like conformation (Fig. 1), as it is visualized by electron microscopy in the case of the preparations of isolated 16S RNA in the compact form (22). If the V- or Y-shaped RNA is inscribed into the 30S particle, the thickened end of the large branch of the RNA participates in the formation of the head, the small branch composes a structural basis of the side bulge, and the bifurcation of the RNA forms a core of the body. (*ii*) All or almost all proteins within the 30S particle possess compact globular conformations, as has been demonstrated in the case of isolated proteins S4, S7, S8, S15, and S16 in solution (23, 25).

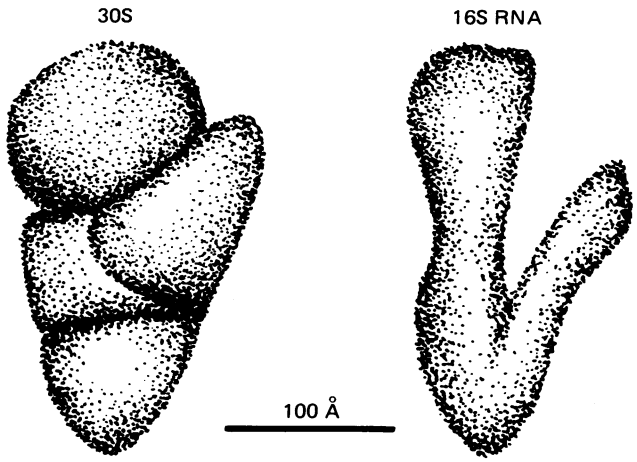

FIG. 1. Morphological models of the ribosomal 30S subunit (26) and its 16S RNA in the compact form (22). The dimensions are from electron microscopy.

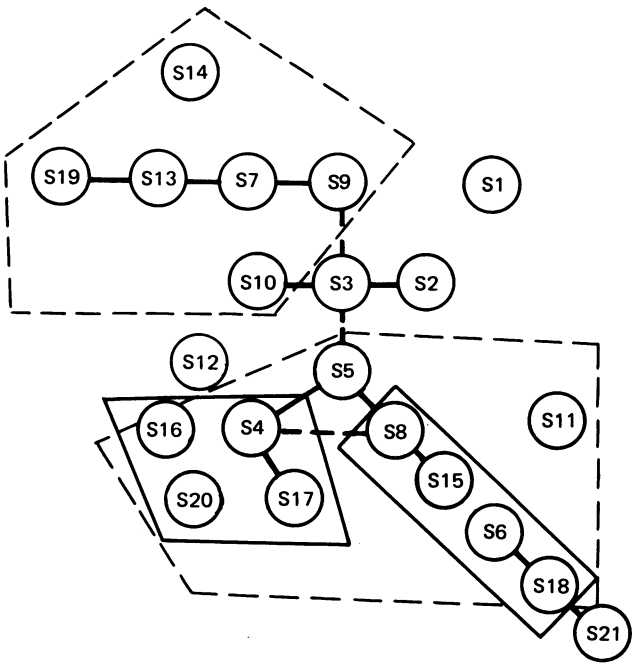

FIG. 2. Scheme of protein neighbors within the ribosomal 30S particle.

Protein–Protein Neighbors. In order to establish pairs of contacting or neighboring proteins within the 30S particle, the following groups of data were used: (*i*) chemical crosslinking of proteins within the particle by bifunctional reagents (for reviews, see refs. 6, 10, 28, and 29); (*ii*) protection of a protein by a neighboring protein from iodination (6); (*iii*) energy transfer between fluorescent-labeled proteins (5); and (*iv*) measurements of distances between deuterated proteins by neutron scattering (7). A pair was taken into further consideration only when no less than three independent indications (either by different techniques or by crosslinking in three independent laboratories) were available. Such reliably determined pairs of contacting or close proteins within the 30S particles were S7/S9, S6/S18, S4/S5, S5/S8, S8/S15, S2/S3, S13/S19, S18/S21, S4/S17, S3/S10, and S7/S13. In addition, proteins in pairs S3/S5, S4/S8, and S3/S9 were also capable of being crosslinked and of protecting each other from iodination, but the distances measured were more than 50 Å.

Summation of the above pairs results in the scheme of protein neighbors given in Fig. 2.

Protein Groups and Ribonucleoprotein Domains. Additional information can be obtained from positions of binding sites of ribosomal proteins on the primary structure of 16S RNA (reviewed in ref. 28) and from the results of RNase fragmentation of the 30S particles (1, 28). These results permit grouping of the ribosomal proteins as shown in Fig. 2 by the solid line (neighboring proteins on the RNA chain) and dashed line (RNase fragmentation).

Thus, all the data reflected in the scheme in Fig. 2 suggest the subdivision of the 30S particle into at least three main ribonucleoprotein domains: (*i*) the most distinct and independent domain containing proteins S9, S7, S13, and S19 and including also S10 and S14; (*ii*) the domain consisting of proteins S4, S16, S17, and S20 and the 5′-half of the RNA; (*iii*) the domain including proteins S8, S15, S6, S18, S21, and, probably, S11, bound near to the middle of the 16S RNA chain.

Positions of the Protein Groups on the Tertiary Structure of RNA. First, it is likely that protein S4 occupies some central position in the 30S particle: (*i*) it is distinguished by the most reported crosslinks and interactions with other proteins (4, 6, 10, 28); (*ii*) it has no antigenic determinants on the surface of the particle and thus is buried inside (30); (*iii*) it is bound simultaneously with several extended but noncontiguous regions of the 16S RNA chain (28, 31, 32). The central position and the unique binding of globular protein S4 to remote long sections of the RNA chain could be realized in the most natural way if it was positioned between the two branches of the Y-shaped RNA molecule, interacting with both the branches. Thus, in constructing the model, we have placed protein S4 and, correspondingly, its neighbors S16, S17, and S20 (Fig. 2), in the bifurcation region of the Y-shaped 16S RNA (Fig. 1). Some chemical data (4, 6) and functional interrelations (see reviews in refs. 10 and 33) suggest that protein S12 is also close to the protein S4 position.

Immunoelectron microscopy results (9–12) were taken into consideration for further positioning of the proteins on the RNA. Unfortunately, however, only in the cases of proteins S8, S9, S13, S14, S20, and, perhaps, S3 and S10, have one or two close antigenic determinants been revealed and the results of the two laboratories more or less coincided (refs. 9 and 10 and refs. 11 and 12). Nevertheless, these results permit definite attribution of S7, S9, S10, S13, S14, and S19 (see Fig. 2) to the head of the 30S particle and, correspondingly, to place this group on the distal part of the longer branch of the Y-shaped RNA (Fig. 1).

Then the group of proteins S8, S15, S6, S18, S21, and S11 (Fig. 2) could be placed on the smaller branch of the RNA (Fig. 1), thus forming the side bulge of the 30S particle. This presumption is supported by Lake's immunoelectron microscopy data revealing the antigenic determinants of proteins S11 and S21, as well as of S15, S6, and S18, on the platform (12).

The data from immunoelectron microscopy (12), x-ray and neutron scattering (34), and assembly interaction with protein S9 (35) suggest that the big protein S1 is located somewhere in the region of the distal part of the smaller branch of the Y-shaped RNA or between it and the head proteins.

Interface Proteins. Analysis of the inhibition of the 30S–50S subunit association by specific antibodies against ribosomal proteins (36) and experiments on chemical crosslinking between components of the two ribosomal subunits (37, 38) have indicated that proteins S6, S9, S11, S12, S14, S16, S18, S20, and, probably, S1 and S3 are more or less facing the 50S subunit and its protuberances within the 70S ribosome. Then, according to the orientation of the 30S subunit relative to the 50S subunit, as determined by electron microscopy of negatively stained (27) or shadow-cast (V. D. Vasiliev, unpublished observations) ribosomes, these proteins must be distributed mainly on the front side, when the smaller branch of the RNA (or the bulge of the 30S particle) is to the right from the larger branch (or from the main body of the particle) (Fig. 1). On the other hand, such proteins as S5, S8, S15, and S17 are back components of the 30S particle in this orientation (Fig. 1).

Model. On the basis of all the above, a model of the quaternary structure of the ribosomal 30S subunit has been built. In constructing the model, the following dimensions of the RNA molecule within the 30S particle have been taken: length, 230 Å; width of the larger branch, 60 Å; width of the smaller branch, 40 Å. Two views of the model are shown in Fig. 3. In Table 1, the radii of the proteins and the coordinates of the centers of the spherical protein globules of the model are given.

At least three reservations must be made. (*i*) Although all the ribosomal proteins have been conditionally modeled here by spheres of the corresponding radii, their real shapes and axial ratios may vary in the wide ranges that are characteristic of

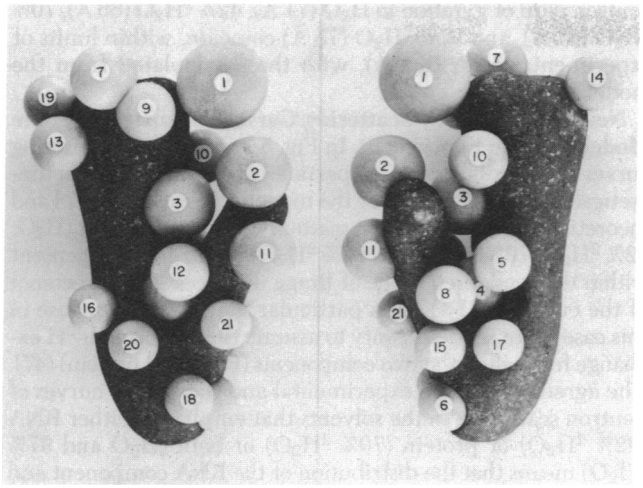

FIG. 3. Model of the quaternary structure of the ribosomal 30S particle photographed from two sides.

compact globular proteins in general. (*ii*) The distances between the proteins in the model reflect only an approximate pattern of their mutual arrangement, without pretensions to absolute accuracy. (*iii*) The positions of several proteins in the model, such as S11 as well as S1, S2, and S21, are more provisional than those of the others.

EXPERIMENTAL TESTING OF THE MODEL

Calculation of Theoretical Scattering Curves for the Model. For calculations, the Y-shaped RNA of the model was composed of identical spheres with a diameter of 10 Å each, in cubic packing. The volume of the RNA was 0.86×10^6 Å^3 which is 2 times more than the dry volume of 16S RNA and is consistent with the experimental value of its hydration (39, 40).

Ribosomal proteins were represented by spheres with radii calculated from molecular weights of the corresponding proteins. Hydration was assumed to be 0.2 g/g. The total volume of the hydrated protein in the model was 510,000 Å^3. It was taken into account that the protein S1 is fractional and is present only in 30% of the ribosomal 30S particles, according to determinations made for our preparations.

Table 1. Diameters and coordinates of the centers of the spherical protein globules (in Å) of the model shown in Fig. 3

Protein	Diameter	*x*	*y*	*z*
S1	55	45	95	220
S2	44	35	120	170
S3	44	50	70	150
S4	42	45	55	100
S5	38	95	45	120
S6	36	55	60	20
S7	40	0	45	230
S8	34	85	80	95
S9	36	10	65	205
S10	35	80	60	185
S11	35	60	125	120
S12	35	5	70	115
S13	34	0	15	195
S14	36	75	0	230
S15	32	80	90	65
S16	31	10	20	95
S17	31	90	45	65
S18	30	20	65	35
S19	32	10	5	225
S20	31	10	45	70
S21	29	15	90	75

The central axis of the large branch of the Y-shaped RNA has x = 45 Å, y = 50 Å, and coincides with the z coordinate, z = 0 at the lowest end of the RNA. The end of the small branch of the RNA has x = 45 Å, y = 135 Å, and z = 160 Å.

The scattering indicatrices for the model at different contrasts (see below) were calculated by the method of spheres (41), taking the corresponding coordinates of the RNA and protein spheres. For calculation of theoretical x-ray scattering curves the electron densities of RNA, protein, and solvent (H_2O) were assumed to be 0.57, 0.44, and 0.34 $e^-/Å^3$, respectively (42). For calculation of neutron-scattering curves, the scattering densities of RNA, protein, and solvent were assumed to be, respectively, $+3.5 \times 10^{10}$, $+1.7 \times 10^{10}$, and -0.56×10^{10} cm^{-2} in H_2O and $+4.4 \times 10^{10}$, $+3.0 \times 10^{10}$, and $+6.2 \times 10^{10}$ cm^{-2} in ^2H_2O (42, 43). In 42 and 70% ^2H_2O the scattering densities of protein and RNA, respectively, were assumed to be close to zero (43).

Measurements of Experimental Scattering Curves for the 30S Particles. Neutron-scattering experiments were made at the Institut Laue-Langevin (Grenoble, France) on the high-flux reactor with the D11 camera (44) at four different contrasts, such as H_2O, 42% ^2H_2O, 70% ^2H_2O, and 97% ^2H_2O. Ribosomal 30S particles of *E. coli* were isolated as described (42). The measurements were done in 90 mM KCl/0.8 mM $MgCl_2$/10 mM Tris·HCl, pH 7.2, prepared in H_2O, 42% ^2H_2O, 70% ^2H_2O, or 97% ^2H_2O. The sample–detector distances were 2.55 and 10.5 m, the wavelengths used were 5.0, 6.4, and 10.0 Å, the range of measured μ was 0.006 to 0.18 Å^{-1} ($\mu = 4\pi/\lambda \sin\theta$, in which 2θ is a scattering angle). The concentrations of the 30S particles were 2–12 mg/ml, in the 1- and 2-mm-thick cells.

Radii of Gyration of the Model at Different Contrasts and Their Comparison with the Experimental Values. In Fig. 4, the solid line represents the dependence of radius of gyration of the model (R_g) on the contrast ($\Delta\rho$), in Stuhrmann's coordinates according to the equation $R_g^2 = R_\infty^2 + \alpha/\Delta\rho - \beta/(\Delta\rho)^2$ for a two-component particle (45), in which R_∞ is a radius of gyration at infinite contrast and α and β are parameters characterizing a mutual arrangement of two components in the particle. The curve shows that the value of α of the model is negative and that of β is relatively small. This indicates that in our model (*i*) the component with higher neutron density

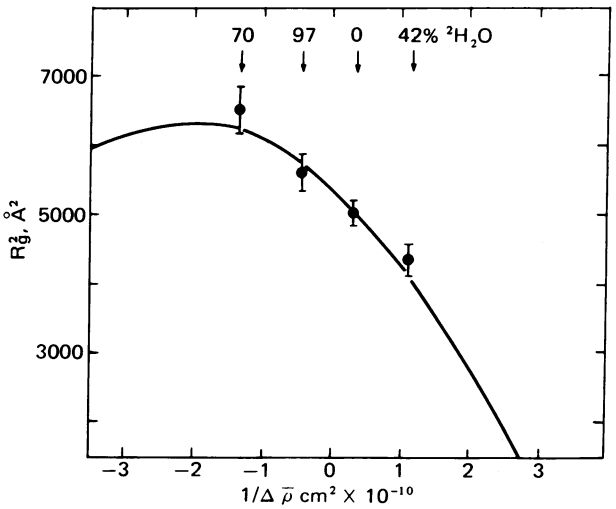

FIG. 4. Dependence of radius of gyration (R_g) on contrast ($\Delta\rho$). Solid line is calculated from the model according to the equation $R_g^2 = 73.7^2 - 874 \times 10^{10}/\Delta\rho - 203 \times 10^{20}/(\Delta\rho)^2$. Symbols are experimental values of R_g^2 for the ribosomal 30S particle at the four contrasts indicated.

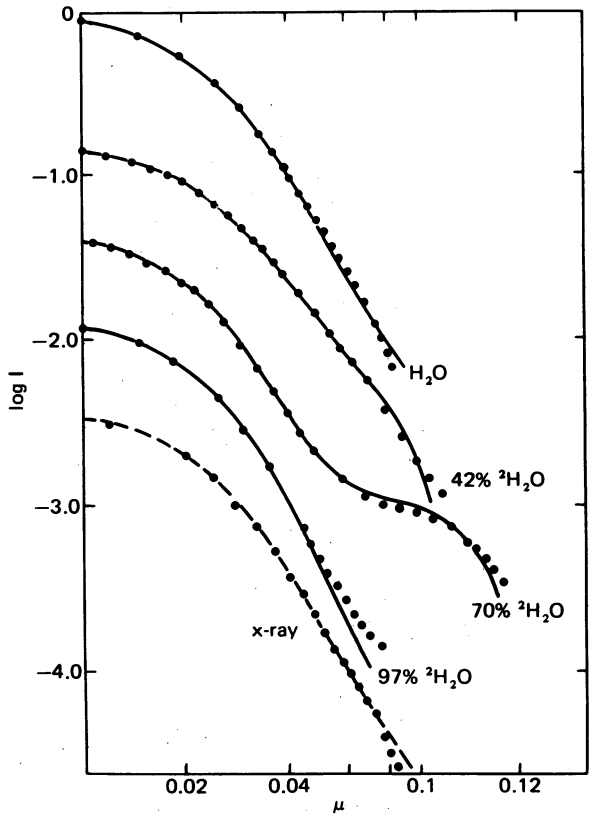

FIG. 5. Comparison of neutron (solid lines) and x-ray (dashed line) scattering curves calculated from the model with the experimental scattering curves (solid circles) for the ribosomal 30S particle.

(RNA) is located closer to the center of the particle than is the less-dense component (protein); and (*ii*) the distance between the centers of gravity of the two components is not great (34 Å). Such a distribution of the RNA and protein components has been experimentally shown for the real 30S ribosomal subunit (39, 46, 47).

Fig. 4 also shows that the absolute experimental values of neutron radii of gyration in H_2O (71 Å), 42% ^2H_2O (66 Å), 70% ^2H_2O (81 Å), and 97% ^2H_2O (75 Å) coincide, within limits of experimental error (±2 Å), with those calculated from the model.

Neutron and X-Ray Scattering Curves: Comparison of the Model with the Experiment. In Fig. 5, experimental scattering curves for the ribosomal 30S particles are compared with theoretical curves calculated for the model. The experimental and theoretical curves of neutron scattering at four contrasts (H_2O, 42% ^2H_2O, 70% ^2H_2O, and 97% ^2H_2O) are in good agreement within the considered range of Bragg distances. The agreement of the curves in H_2O has a particular significance because in this case there is no necessity to assume the uniform H–^{2}H exchange for each of the two components (RNA and protein) (47). The agreement of the experimental and theoretical curves of neutron scattering in the solvents that emphasize either RNA (42% ^2H_2O) or protein (70% ^2H_2O) or both (H_2O and 97% ^2H_2O) means that the distribution of the RNA component and the protein molecules in the model does not contradict the experiment, down to Bragg distances of about 40 Å (for protein) or 55 Å (for RNA).

The 30S particles of *E. coli* ribosomes have been studied by x-ray scattering technique in several laboratories (42, 48–51). The comparison of the experimental curve (45) with the theoretical one calculated from the model again shows good agreement (Fig. 5). Hence, the model does not contradict the well-known x-ray scattering data.

Theoretical Scattering Curves for Different Models of Ribosomal Protein Topography: Comparison with the Experimental Curve. Theoretical curves of neutron scattering for some models of ribosomal protein topography proposed earlier by other authors (2–4, 8) have been also calculated as described above and are presented in Fig. 6. All the curves calculated for the different models of protein topography proposed earlier diverge from the experimental neutron-scattering curve for the protein component of the ribosomal 30S particle (scattering in 70% ^2H_2O).

We thank Dr. G. Zaccai (Institut Laue-Langevin, Grenoble, France) for help in neutron-scattering measurements and Dr. B. Jacrot, of the same Institute, for discussions and advice. We are also very grateful to Prof. I. M. Gelfand for giving us an excellent opportunity to discuss the paper at his Cell Biology Seminars at the Moscow State University.

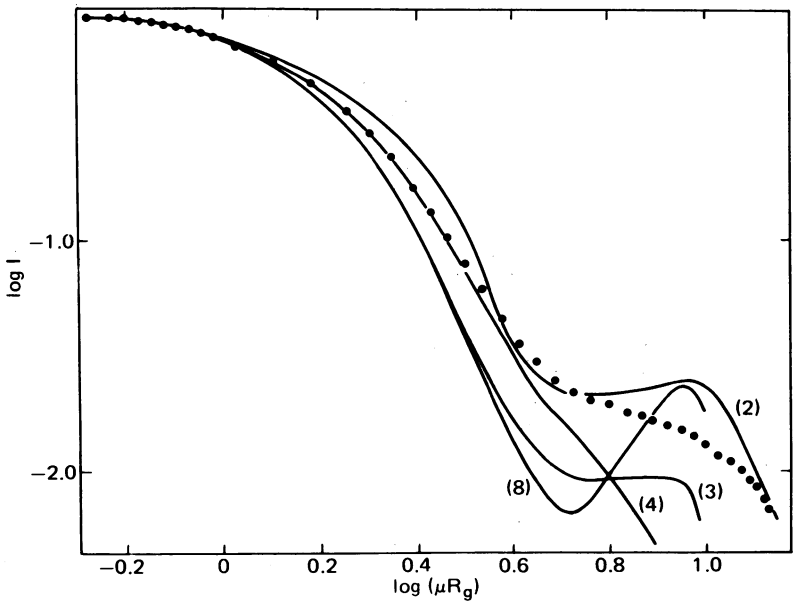

FIG. 6. Comparison of scattering curves calculated for the earlier reported models of the protein topography of the 30S particle (solid lines with corresponding references) with the experimental neutron scattering curve (solid circles) for the protein component of the ribosomal 30S particle (in 70% ^2H_2O where only the protein component is revealed). The radii of gyration calculated for the models are 91 Å (2), 50 Å (3), 58 Å (4), and 55 Å (8).

1. Morgan, J. & Brimacombe, R. (1973) *Eur. J. Biochem.* **37,** 472–480.
2. Bollen, A., Cedergren, R. J., Snakoff, D. & Lapalme, G. (1974) *Biochem. Biophys. Res. Commun.* **59,** 1069–1078.
3. Sun, T.-T., Heimark, R. L. & Traut, R. R. (1975) *Mol. Cell. Biochem.* **6,** 33–41.
4. Sommer, A. & Traut, R. R. (1975) *J. Mol. Biol.* **97,** 471–481.
5. Huang, K.-H., Fairclough, R. H. & Cantor, C. R. (1975) *J. Mol. Biol.* **97,** 443–470.
6. Changchien, L.-M. & Craven, G. R. (1977) *J. Mol. Biol.* **113,** 103–122.
7. Langer, J. A., Engelman, D. M. & Moore, P. B. (1978) *J. Mol. Biol.* **119,** 463–485.
8. Cornick, G. G. & Kretsinger, R. H. (1977) *Biochim. Biophys. Acta* **474,** 398–410.
9. Tischendorf, G. W., Zeichhardt, H. & Stöffler, G. (1975) *Proc. Natl. Acad. Sci. USA* **72,** 4820–4824.
10. Stöffler, G. & Wittmann, H. G. (1977) in *Molecular Mechanisms of Protein Biosynthesis,* eds. Weissbach, H. & Pestka, S. (Academic, New York), pp. 117–202.
11. Lake, J. A. & Kahan, L. (1975) *J. Mol. Biol.* **99,** 631–644.
12. Lake, J. A. (1978) in *Advanced Techniques in Biological Electron Microscopy,* ed. Koehler, J. K. (Springer, Berlin), Vol. 2, pp. 173–211.
13. Gaffney, P. T. & Craven, G. (1978) *Proc. Natl. Acad. Sci. USA* **75,** 3128–3132.
14. Engelman, D. M., Moore, P. B. & Schoenborn, B. P. (1975) *Proc. Natl. Acad. Sci. USA* **72,** 3888–3892.
15. Moore, P. B., Langer, J. A., Schoenborn, B. P. & Engelman, D. M. (1977) *J. Mol. Biol.* **112,** 199–234.
16. Paradies, H. H. & Franz, A. (1976) *Eur. J. Biochem.* **67,** 23–29.
17. Österberg, R., Sjöberg, B., Garrett, R. & Littlechild, J. (1977) *FEBS Lett.* **73,** 25–28.
18. Österberg, R., Sjöberg, B. & Littlechild, J. (1978) *FEBS Lett.* **93,** 115–119.
19. Gulik, A., Freund, A. M. & Vachette, P. (1978) *J. Mol. Biol.* **119,** 391–397.
20. Rohde, M. F., O'Brien, J., Cooper, J. & Aune, K. C. (1975) *Biochemistry* **14,** 1079–1087.
21. Giri, L. & Franz, A. (1978) *FEBS Lett.* **87,** 31–36.
22. Vasiliev, V. D., Selivanova, O. M. & Koteliansky, V. E. (1978) *FEBS Lett.* **95,** 273–276.
23. Serdyuk, I. N., Zaccai, G. & Spirin, A. S. (1978) *FEBS Lett.* **94,** 349–352.
24. Khechinashvili, N. N., Koteliansky, V. E., Gogia, Z. V., Littlechild, J. & Dijk, J. (1978) *FEBS Lett.* **95,** 270–272.
25. Gogia, Z. V., Venyaminov, S. Yu., Bushuev, V. V., Serdyuk, I. N., Lim, V. I. & Spirin, A. S. (1979) *FEBS Lett.,* in press.
26. Vasiliev, V. D. (1974) *Acta Biol. Med. Germ.* **33,** 779–793.
27. Lake, J. A. (1976) *J. Mol. Biol.* **105,** 131–159.
28. Brimacombe, R., Nierhaus, K. H., Garrett, R. A. & Wittmann, H. G. (1976) in *Progress in Nucleic Acid Research and Molecular Biology,* ed. Cohn, W. E. (Academic, New York), Vol. 18, pp. 1–44.
29. Expert-Bezancon, A., Barritault, D., Milet, M., Guerin, M.-F. & Hayes, D. H. (1977) *J. Mol. Biol.* **112,** 603–629.
30. Winkelmann, D. & Kahan, L. (1978) *Fed. Proc. Fed. Am. Soc. Exp. Biol.* **37,** 1739.
31. Ehresmann, B., Backendorf, C., Ehresmann, C. & Ebel, J. P. (1977) *FEBS Lett.* **78,** 261–266.
32. Cole, M.D., Beer, M., Koller, Th., Strycharz, W. A. & Nomura, M. (1978) *Proc. Natl. Acad. Sci. USA* **75,** 270–274.
33. Kurland, C. G. (1977) in *Molecular Mechanisms of Protein Biosynthesis,* eds. Weissbach, H. & Pestka, S. (Academic, New York), pp. 81–116.
34. Laughrea, M. & Moore, P. B. (1978) *J. Mol. Biol.* **122,** 109–112.
35. Laughrea, M., Engelman, D. M. & Moore, P. B. (1978) *Eur. J. Biochem.* **85,** 529–534.
36. Morrison, C. A., Garrett, R. A., Zeichhardt, H. & Stöffler, G. (1973) *Mol. Gen. Genet.* **127,** 359–368.
37. Sun, T.-T., Traut, R. R. & Kahan, L. (1974) *J. Mol. Biol.* **87,** 509–522.
38. Bäumert, H. G., Sköld, S.-E. & Kurland, C. G. (1978) *Eur. J. Biochem.* **89,** 353–359.
39. Serdyuk, I. N. (1979) *Methods Enzymol.* **59,** 750–775.
40. Serdyuk, I. N. (1979) *Mol. Biol. (USSR)* **13,** 965–982.
41. Rolbin, Yu. A., Kayushina, R. L., Feigin, L. A. & Shchedrin, V. M. (1973) *Kristallografiya* **18,** 701–705.
42. Serdyuk, I. N. & Grenader, A. K. (1977) *Eur. J. Biochem.* **79,** 495–504.
43. Jacrot, B. (1976) *Rep. Progr. Phys.* **39,** 911–953.
44. Ibel, K. (1976) *J. Appl. Crystallogr.* **9,** 630–643.
45. Stuhrmann, H. B. (1974) *J. Appl. Crystallogr.* **7,** 173–178.
46. Beadry, P., Peterson, H. V., Grunberg-Manago, M. & Jacrot, B. (1976) *Biochem. Biophys. Res. Commun.* **72,** 391–397.
47. Stuhrmann, H. B., Koch, M. H., Parfait, R., Haas, J., Ibel, K. & Crichton, R. R. (1978) *J. Mol. Biol.* **119,** 203–212.
48. Kayushina, R. L. & Feigin, L. A. (1969) *Biofizika* **14,** 957–962.
49. Hill, W. E., Thompson, J. D. & Anderegg, J. W. (1969) *J. Mol. Biol.* **44,** 89–102.
50. Smith, W. S. (1971) Dissertation (Univ. Wisconsin, Madison, WI).
51. Hill, W. E. & Fessenden, R. J. (1974) *J. Mol. Biol.* **90,** 719–726.